European Journal of Remote Sensing - 2014, 47: 477-496
doi: 10.5721/EuJRS20144727
Received 24/03/2014, accepted 16/05/2014

European Journal of Remote Sensing
An official journal of the Italian Society of Remote Sensing

www.aitjournal.com

Development of a software to optimize and plan the acquisitions from UAV and a first application in a post-seismic environment

Valerio Baiocchi[1*], Donatella Dominici[2], Maria Vittoria Milone[1] and Martina Mormile[1]

[1]Department of Civil, Construction and Environmental (DICEA), La Sapienza University, Rome, Italy
[2]Department of Civil, Construction-Architecture and Environmental (DICEAA)
University of L'Aquila, L'Aquila, Italy
*Corresponding author, e-mail address: valerio.baiocchi@uniroma1.it

Abstract
An Unmanned Aerial Vehicle (UAV) is an aircraft without a human pilot on board. UAVs allow close-range photogrammetric acquisitions potentially useful for building large-scale cartography and acquisitions of building geometry. This is particularly useful in emergency situations where major accessibility problems limit the possibility of using conventional surveys. Presently, however, flights of this class of UAV are planned based only on the pilot's experience and they often acquire three or more times the number of images needed. This is clearly a time-consuming and autonomy-reducing procedure, which is certainly detrimental when extensive surveys are needed. For this reason new software, to plan the UAV's survey will be illustrated.

Keywords: Earthquake, emergency mapping, flight planning, photogrammetry, UAV.

Introduction
Unmanned Aerial Vehicle (UAV) is aircraft usually remotely piloted from a ground station; with low-altitude flight, they represent the last frontier for the survey of the territory. The possibility to install different sensors makes them very useful for various applications both in urban and rural areas, such as the analysis of environmental risk or the estimation of the changes of land use. This innovative methodology is subject to increasing scientific interest, but the actual possibilities of its application are yet to be fully verified.
To evaluate and preliminarily assess the photogrammetric potentialities of these systems, they were tested and applied for a documentation of the damage caused in the historic center of L'Aquila by the earthquake of April 2009. The scenario of this event is very specific: on the night of April 6, 2009, an earthquake of MW 6.3 magnitude occurred in the Abruzzo region, in the central Italy; the hypocenter was estimated by the National Institute for Geophysics and Vulcanology (INGV) at 42.35° N and 13.38° E, at a 9.5 km depth; moreover, at least more than three month of pre-seismic events preceded the main shock,

and aftershocks continued for at least six months. The epicenter of the main shock was nearby the historic center of L'Aquila, the capital of the Abruzzo region which, together with surrounding villages, suffered the most damage. The foreshocks had been occurring since December 2008; more than thirty of the foreshocks and aftershocks had a Richter magnitude greater than 3.5. All of the masonry buildings, including the traditional palaces and high-density residential areas in the old city center, suffered severe damage, and many of them suffered partial collapse. Detailed surveying of all buildings is needed to plan the reconstruction of each structure, but the survey activities have just begun, using traditional geomatic instruments like total stations, close range photogrammetry, LASER scanners and deformation-monitoring instruments. Even if all of these techniques could perfectly fulfill many crucial post-hazard needs, they would still be limited in many cases. Most of the difficulties are related to the morphologic and architectural accessibility, problems typical of post-disaster scenarios. During a post-seismic period, surveying with classical topographic instruments is difficult as well as complex due to the possible residual danger in the area. Other methodologies like aerial photogrammetry are surely less dangerous but, in most cases, would not produce detailed and accurate information about the damaged structures, especially for the facades. On the other hand, the use of UAVs could easily bypass many of these problems [Eisenbeiss et al., 2010]. For example, an UAV has no accessibility problems indeed it can access virtually any place also in inside. In particular, in the field of civil protection, where the conditional priority is the safety of the operators, these platforms are used for observation and data collection in areas affected by earthquakes, landslides, subsidence, and avalanches, and for the control of forests and prevention of summer fires without metric requirements.
One particular interest is the UAV's potential ability to produce photogrammetric three-dimensional acquisition.

State of the art

Different research groups are involved in studies related to various aspects of UAVs. Their contributions can be itemized under the following main topics: performance optimization, attitude control, flight control and navigation, path planning and obstacles avoidance, obviously the last argument is the most pertinent to the present research.
A number of contributions are related to the UAV performance optimization; in Erbil et al. [2013] the length of touring time a UAV requires to navigate waypoints was minimized using a model built by solving the travelling salesman problem (TSP). Other authors studied the design and deployment of minimal protective system for a multi-rotor UAV to cater for changes in legislation.
Several groups contributed in the aspect of UAV attitude control, in Conte et al. [2008] an on-board attitude stabilization controller for a quadrotor was developed for various applications. Similarly, in [Alpen et al., 2009], a controller was designed using the Active Disturbance Rejection Control technique to regulate the velocity and attitude of an UAV in various wind turbulence conditions.
Regarding more strictly flight control and navigation systems, different approaches are being studied like cost-effective implementation for indoor application. In another development, illustrated a Real-Time Indoor Autonomous Vehicle Test Environment; similarly, How et al. [2008] explored a method that integrates three-dimensional (3D) point cloud data, two-

dimensional (2D) digital camera data and data from an Inertial Measurement Unit (IMU) to provide accurate position and attitude determination of UAV.
Numerous contributions concern more specifically the path planning and obstacle avoidance, e.g, an innovative evolutionary algorithm was utilized in Xiong et al. [2011] and Nikolos et al. [2003], to design an intelligent path planner for UAV autonomous navigation. A real-time path-planning algorithm was instead developed and tested in Rathbun et al. [2002] for a quadrotor UAV base on Rapidly-exploring Random Tree approach (RRT). Similarly, a low-complexity, accurate and reliable scheme for motion field estimation was developed, using UAV navigation videos in Hrabar [2008], and used to determine the range map for objects in the scene.
Extensive literature concerns also the specific subject of guidance that has strong connections with flight planning; in fact this latter is a dynamic process of directing an object toward a given point that may be stationary or moving. For example numerous trajectory generation methods for rotorcraft UAVs have been demonstrated in Astrov et al. [2010] and Mellinger et al. [2011].
UAV applications for geomatics, anyway are currently especially used in areas that may be too dangerous for manned aircraft or other surveys; mainly in case of natural emergencies, high-resolution images become a fundamental tool for the assessment of damages impacts on infrastructures and strategic areas. In fact information on the road network conditions, the damage in infrastructures, which could potentially increase the hazard (dams, dikes, bridges), are not always guaranteed by high-resolution images [Bendea et al., 2008].

Aim of software UP23d

A correct photogrammetric survey needs a suitable number of high-quality acquisitions with the correct geometry [Ioannis et al., 2003]. To assure this quality, the whole flight and, thus, the waypoints (point when the UAV take the images) have to be spatially distributed, maintaining definite geometric characteristics as equal and correct air base and correct interaxes [Kraus, 1994]. One important characteristic of planning is the expected average scale of the frame, defined as the mean relation between the dimension of an element in the image and the actual dimension of the element on the ground. Due to the fact that the terrain usually does not have a flat morphology, the distance between each point of the image and the waypoint is not the same; thus, an average value of this distance is used to evaluate the scale. The average scale is used as a guideline to correctly generate maps at the required accuracy. This logic is undisputed for metric cameras on aerophotogrammetric flights; we want to determine if this approach could also be correctly implemented for a multirotor UAVs using non-metric camera. The goal is to obtain only the frames needed to reconstruct the stereoscopy and to obtain geometrically correct reconstructions of the objects observed to build a Digital Surface Model (DSM); for this reason, an original software (UP23d: UAVs planner to 3-dimensional acquisitions) was developed by the authors to model the flight plan of the UAV for acquisition optimization and to simultaneously evaluate this approach for a multirotor UAVs using commercial cameras. As it is well known DSM, is a digital model or 3D representation of a terrain's surface including elevation of object as buildings where present and elevation of ground if no object is present on the ground itself. As a more recent development, the package was modified to allow the planning of monoscopic acquisitions when only the production of orthophoto is needed. The UP23d software at the present state of development operates as shown in Figure 1. The software UP23d requires as input data the size, shape and position of the area to be acquired, the

optic parameters of the camera installed on the UAV and the desired final scale of the acquisitions. From these first input data the package suggest a flight altitude, which is proposed to the user which is free to edit if it's not suitable for the area to be investigated (for example, there is an obstacle with a height near to the estimated flight elevation). Once estimated the flight height and consequently the final scale obtainable (hypnotized considering as guideline the classical aerophotogrammetric scale parameters), the values of endlap and across sidelap have to be inserted in the software to allow the evaluation of the air base needed to assure a correct stereoscopic reconstruction. After this step, the software proceeds to the calculation of waypoints and footprint of each acquisition. As output the software returns the coordinates of the points where the UAVs has to stop to acquire the images; also a vector files of polygons that shows footprint of each frame is produced.

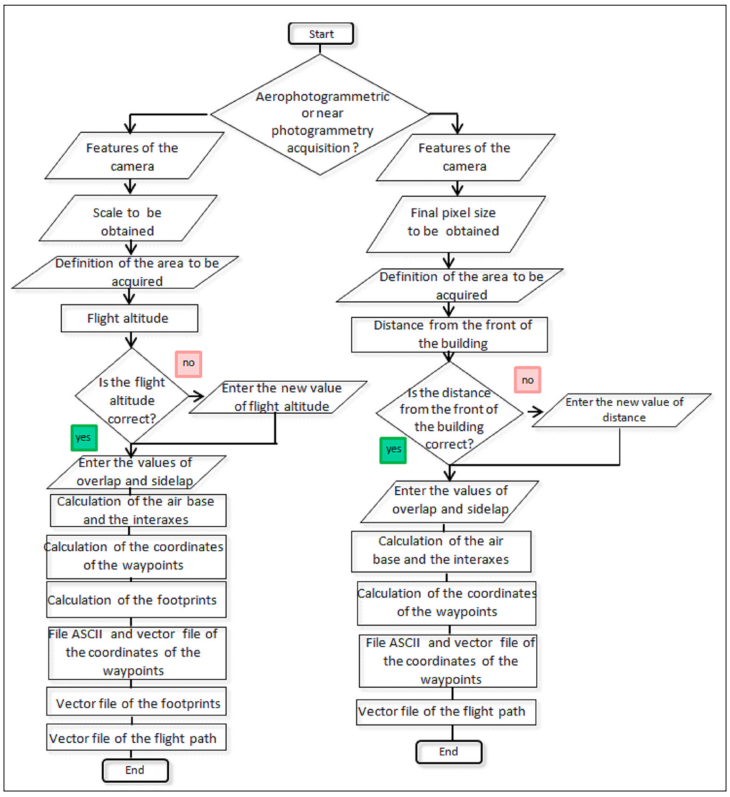

Figure 1 - Flow chart of the UP23d software.

At its end the program provide a report file, which also contains the intermediate results that were estimated during its execution. Vector files can then be loaded into a GIS environment, as the open source Q-Gis, that allow overlapping to aerial or satellite orthophoto or to existing raster or vector cartography. In a post-seismic environment, UAVs can be also particularly useful for acquiring the facades of buildings in non-accessible areas for photogrammetry acquisitions [Stefanik et al., 2011; Novelli et al., 2012]. For this reason also UP23d was upgraded to manage close range photogrammetry acquisitions; in this case, the package

operates in a slightly different way, as shown in Figure 1. As for the aerophotogrammetric survey, the size of the area to be acquired is entered as input data, the optic parameters of the camera installed on the UAV and the dimensions of the pixel in the acquisitions are needed.

Tests performed

To realize this experiment a typical Italian square with historic-monumental buildings was chosen: "Piazza Palazzo" in L'Aquila city. Its dimensions are approximately 60 meters long to 38 meters wide covering a total area of 2500 square meters and surrounded by the public library, the city hall "Palazzo Margherita" with its 40 m height bell tower.
This experiment in the historic center of L'Aquila for this project is the result of collaboration between the Faculties of Engineering of L'Aquila and Rome universities, and the IPT Company of Rome, that gently provided a Mikrokopter platform in Okto configuration (Fig. 2). The choice of this platform was made trying to achieve good flying characteristics that can allow an optimum stability even in presence of wind or other no optimal climatic conditions and according to the payload specified by the manufacturer, which allows carrying a reflex digital camera; in particular, a Canon EOS 550D (focal lens: 18 mm) equipped with a wireless video transmission to the ground was chosen to allow a better control of the flight and acquisitions in real time.

Figure 2 - Mikrokopter platform in Okto configuration.

UAVs can operate in an autonomous, preplanned flight or in a remote-piloting modality; through the latter method, the UAV pilot, based on his experience, decided to execute a flight from a height of 60 m with full coverage of the square but with only spot acquisitions because the drone showed some instability, probably due to particular meteorological conditions (Fig.3, Fig.4). The entire route taken by the UAV was continuously monitored using wireless video transmission, so the sequence of shots made by the camera was planned and controlled manually by the operators. During the flight the pilot covered the area with

15 acquisitions while our software estimated a need for only six acquisitions (Fig. 5).

Figure 3 - Acquisitions made by the UAV pilot (Piazza del Palazzo field test).

Figure 4 - Acquisitions made by the UAV pilot with the footprint for each acquisitions (Piazza del Palazzo field test).

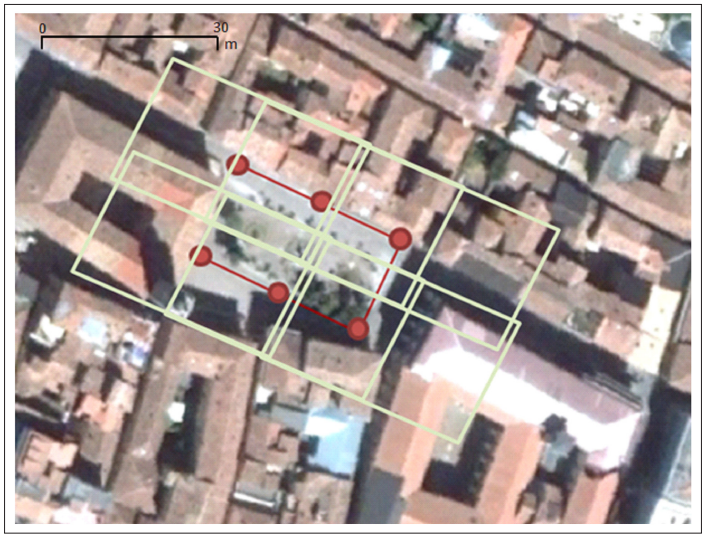

Figure 5 - Vectorial path and footprint plotted by the UP23d software, considering a flight altitude of 60 m, 60% endlap, 20% sidelap, air base of 70 m and interaxes 45 m (Piazza del Palazzo field test).

As previously noted, 15 acquisitions over an area of 60 m x 40 m are probably redundant, especially considering the limited autonomy of the UAVs. With our software we also simulated a flight from a height of 80 m and it evaluated that only two shots were needed (Fig. 6). We would like to underline that this is only an initial experiment; these results will certainly need to be verified.

Figure 6 - Vectorial path and footprint plotted by the UP23d software, considering a flight altitude of 80 m, 60% endlap, 20% sidelap, air base of 40 m and interaxes 54 (Piazza del Palazzo field test).

In Figure 5 and Figure 6, we can see the acquisitions planned by the software for the two different flight heights; we can also observe the drastic reduction in the number of images needed. The table 1 representing a summarizing table that contains the main features of each survey analyzed.

Table 1 - Characteristic of path simulation by the software UP23d.

	First Path Simulation	Second Path Simulation
Flight altitude (m)	60	80
Endlap	60%	60%
Sidelap	20%	20%
Air Base (m)	70	40
Interaxes (m)	45	54
Number of waypoints	6	2

The first tests on the DSM automatic extraction confirmed that the number of acquisitions executed by the pilot was extremely redundant; in fact, the baseline between consecutive acquisitions seems to be too short, resulting in approximately seven useless acquisitions for DSM extraction.
The extraction of a DSM from a photogrammetric survey requires at least one pair of frames with a minimum overlap of 60%, as the stereoscopy required for 3-D restitution is realized only in this area of overlap. In this case, we have considered the two acquisitions made by the pilot UAVs that come closest to those indicated by the UP23d software (Fig.7).

Figure 7 - The two acquisitions made by the pilot UAVs chosen for the extraction of DSM (Piazza del Palazzo field test).

It has to be underlined that anyway the stereopair chosen was the only suitable after examining and selecting more than fifteen acquisitions taken during two different campaigns. Most part of the acquired images was unsuitable because not acquired with the correct geometry or blurred for reduced stability of the UAV. The selection of the unblurred images is actually being studied from other research groups; the correct planning can avoid acquiring geometrically useless images.

To take advantage of the stereoscopic vision for the extraction of DSM, the two frames must be relatively oriented by the collimation of some tie points in order to reassemble the mutual position when shooting. In fact a tie is a point in a digital image that represents the same location in an adjacent image, and can be used to link images. This operation is called relative orientation. It is also necessary to reconstruct the geometry of the two images in relation to the surface, calculating the position and orientation of the camera relative to the ground at the time the frames were acquired [Neininger et al., 2011; Costantino et al., 2013]. This operation, called absolute orientation, is also part of the external orientation and is performed starting from the identification and collimation on each frame of the Ground Control Point (GCP), linking the collimated points with the relative ground coordinates. In the case of Piazza Palazzo, an area of about 60 m x 38 m, we chose instead to use 21 control points in total, corresponding in part to natural points on the masonry elements or edges already present in the square, and in part to new points with photogrammetric signals on the road, along the perimeter. The 21 points were acquired by a differential GNSS RTK (Real Time Kinematic) receiver, using classical topographic instruments when GPS survey was impossible. Processing was performed with the software Geomatics 2013 by PCI. The processing of aerial images acquired with the UAV and the extraction of their metric characteristics requires some preliminary steps, such as camera calibration. PCI Geomatics 2013 does not perform automatically calibration; the parameters must be entered manually. For this reason, the camera calibration has been realized through the use of software Photomodeler and predetermined calibration sheet (Fig.8), which allowed obtaining the internal orientation and lens distortion parameters. The following steps were performed using standard procedures and led quickly to the extraction of the DSM.

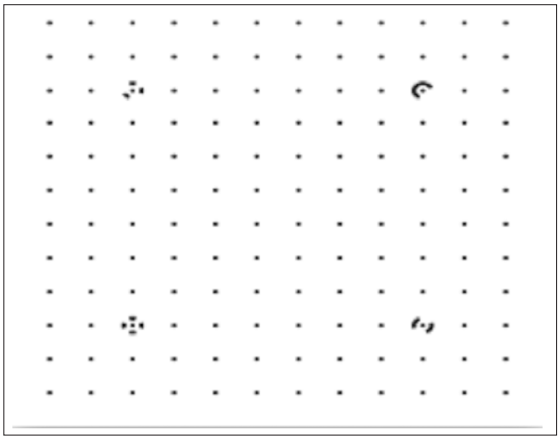

Figure 8 - The preprinted sheet for the calibration with camera CANON EOS 550D.

Are represented in the Table 2 and Table 3 the residual obtained after the orientation.
The impressive precision that characterizes the obtained DSM is clearly demonstrated in Figure 9; in fact, objects with little elevation are visible: note, in the center of the image, the circular boardwalk that is only 10 cm higher than the surrounding ground. On the same area a LIDAR survey, acquired on 04 April 2009 using the ALTM Airborne LASER Terrain Mapper Systems Gemini, was available. In the Table 4 are showed technical characteristic. This test the operating altitude was 1300 m, and set of 1060 LIDAR points were available to check the accuracy of UAV DSM. Comparing the height differences of the DSM obtained with LIDAR points, we observe some local effects, like as systematic shift (around 0.8 m) in the SW corner of the square. This could be caused by a real deformation of the ground, soil movement after the earthquake, or a simple correlation bias of DSM extraction software caused by shadows. From this introductory validation, a maximum difference of around one meter was observed, and this value is compatible with the expected accuracy, but to determine the cause of this deformation, a more detailed topographic survey, such as a geometric leveling, must be performed [Barbarella et al., 1984] , but it's beyond the goal of the present paper.

Table 2 - GCP residuals.

ID POINT	IMG1			IMG2		
	RESIDUAL	RES X	RES Y	RESIDUAL	RES X	RES Y
1	0.021	0.021	-0.004	0.042	0.011	0.041
2	0.078	0.016	0.077	0.009	0.003	0.009
3	0.074	0.071	-0.021	0.042	0.016	0.038
4	0.054	0.016	-0.052	0.101	-0.23	-0.098
5	0.061	-0.056	-0.024	0.098	-0.087	-0.045
6	0.033	-0.029	-0.015	0.014	-0.013	-0.003
7	0.035	0.000	0.035	0.012	0.004	0.011
8	0.058	-0.030	0.050	0.020	-0.017	0.010
9	0.081	0.077	0.025	0.083	0.077	0.031
10	0.016	-0.015	-0.004	0.054	0.032	0.044
11	0.061	0.046	0.040	0.016	0.010	0.012
12	0.056	0.024	-0.051	0.074	-0.012	-0.073
13	0.137	-0.029	-0.134	0.049	0.048	-0.006
14	0.018	0.015	0.009	0.129	0.062	0.144
15	0.117	-0.105	0.052	0.148	-0.120	0.086
16	0.035	0.117	0.009	0.054	-0.103	0.035
17	0.018	0.061	0.025	0.064	0.071	-0.024
18	0.058	0.033	0.012	0.074	-0.085	0.007
19	0.078	-0.030	0.011	0.034	0.040	-0.011
20	0.080	0.010	-0.006	0.056	-0.029	0.044
21	0.023	0.062	-0.045	0.037	0.077	-0.003

Table 3 - Tie points residuals.

ID POINT	TIE POINT		
	RESIDUAL	RES X	RES Y
1	0.035	0.030	-0.017
2	0.027	0.024	-0.014
3	0.026	-0.023	0.013
4	0.026	-0.022	0.013
5	0.019	-0.017	0.009
6	0.017	-0.014	-0.009
7	0.016	-0.014	0.008
8	0.016	-0.014	0.008
9	0.016	-0.014	0.008
10	0.015	-0.014	0.007
11	0.015	-0.014	-0.007
12	0.014	-0.012	0.007
13	0.013	0.011	-0.007
14	0.012	0.010	-0.006
15	0.011	0.010	-0.006
16	0.011	-0.009	0.005
17	0.010	-0.009	0.005
18	0.010	0.009	-0.005
19	0.010	-0.009	0.005
20	0.010	-0.009	0.005
21	0.010	0.008	-0.005
22	0.010	0.008	-0.005
23	0.009	-0.008	0.005
24	0.009	0.008	-0.005
25	0.009	-0.008	0.004
26	0.007	-0.007	0.003
27	0.007	0.006	-0.003
28	0.007	0.006	-0.004
29	0.006	0.005	-0.003
30	0.006	0.005	-0.003
31	0.006	0.005	-0.003
32	0.006	-0.005	-0.003
33	0.006	-0.005	-0.003
34	0.006	0.005	0.003
35	0.005	0.005	-0.003
36	0.005	-0.005	0.002
37	0.005	-0.004	0.002
38	0.005	0.004	-0.002
39	0.004	0.003	-0.002
40	0.004	0.003	-0.002
41	0.003	-0.003	0.002
42	0.003	0.003	-0.002
43	0.003	0.002	-0.001
44	0.002	-0.002	0.001
45	0.002	0.002	-0.001
46	0.003	0.002	-0.001

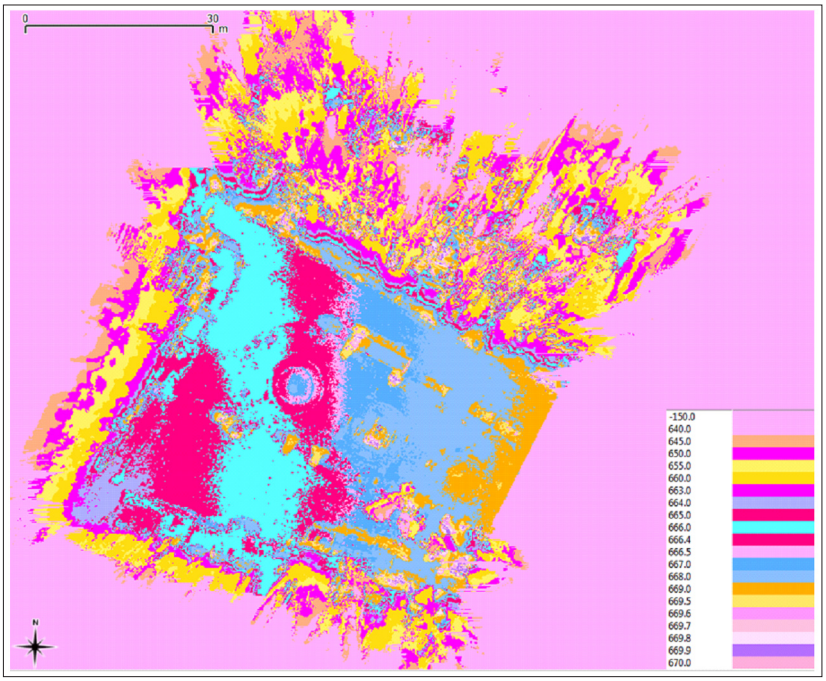

Figure 9 - DSM resulting from the process of automatic extraction.

Table 4 - Technical characteristics of LIDAR.

	ALTM Airborne LASER Terrain Mapper Systems Gemini
Laser repetition rate	33 - 167 kHz
Operating altitude	80 to 4,000 m (higher altitude optional)
Horizontal accuracy	1/11,000 x altitude; ±1-sigma*
Elevation accuracy	5 - 10 cm typical; ±1-sigma
Range capture	Up to 4 range measurements for each pulse, including last
Intensity capture	4 intensity readings with 12-bit dynamic range for each measurement
Scan frequency	Variable to 100 Hz
Scan angle	Variable from 0 to ±25°, in increments of ±1°
Spot distribution	Sawtooth, uniform spot spacing across 96% of scan
Scanner product	Scan angle x scan frequency ≤1,000
Roll compensation	5 Hz update rate (Scan angle + roll comp. angle = 30°, e.g., ±20° scan allows ±10° compensation)
Swath width	Variable from 0 to 0.93 x altitude (m)
Beam divergence	Dual divergence 0.15/0.25 mrad or nominal (1/e full angle) 0.80 mrad
Laser classification	Class IV (FDA 21 CFR)
Position orientation	Applanix - POS\AV including internal system 12-channel dual-frequency 10 Hz GPS receiver

Other blunders could be caused by the presence or absence of vehicles or other mobile obstacles (Fig.10) during the two acquisitions or different responses to foliage on the trees. In fact, LIDAR is usually filtrated from the first echoes due to the presence of leaves, while photogrammetric DSM considers the height of the trees. Because there is no certainty of the potential presence and position of cars and other structures at the time of the LIDAR survey, we decided to perform the tests only on a snipped of the available data, focusing on the inner part of the square (251 points) (Fig. 11).

Figure 10 - GRID from LIDAR points used where mobile obstacles are evident (http://www.pcn.minambiente.it/GN).

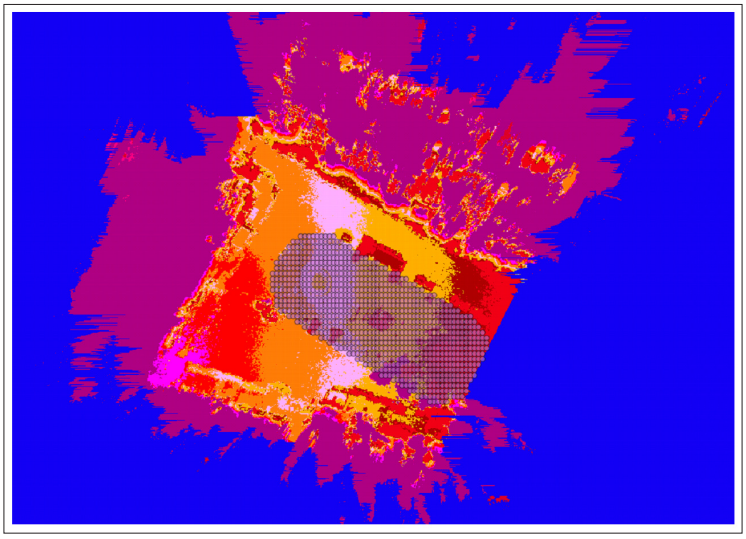

Figure 11 - Overlap of the LIDAR points on the DSM, considering only the square.

The results obtained were then plotted in a histogram, as shown in Figure 12 where it's possible to observe a significant fit with an error distribution compatible with the expected accuracy of LIDAR; a slight asymmetry of the distribution can be due to the yet declared different responses to foliage on the trees of the two techniques.

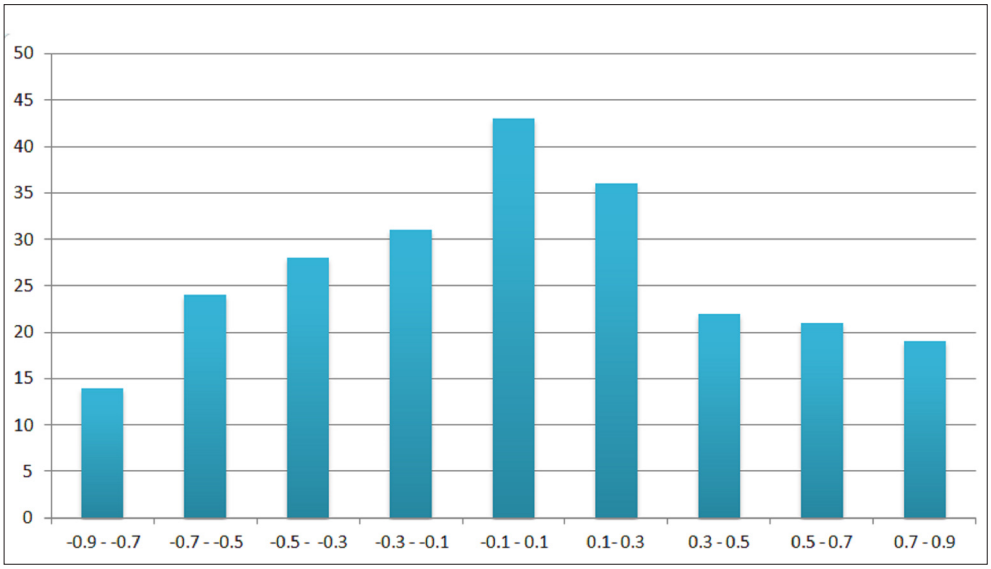

Figure 12 - Distribution of differences (m) between photogrammetric DSM and LIDAR points.

To better evaluate the accuracy of the DSM, we performed a LASER scanning survey using a Riegl Z210i LASER scanner that can be considered a medium-accuracy class instrument.
Table 5 displays the main technical characteristics of the instrument. We compared the differences in height of the DSM obtained and the LASER points (georeferenced in the same reference system of photogrammetric data) (Fig.13), considering a set of 9427 points. The results obtained were then plotted in a histogram, and they are shown in Figure 14.

Table 5 - Technical characteristics of the LASER scanner.

	Riegl Laser Scanner Z210i
Field of view	Vertical: 90° Horizontal: 360°
Maximum range	1000 m
Digital camera	External calibrated mount
Resolution range	5 mm
Resolution	0.002°
Beam divergence	0.25 mrad
Data acquisition rate	12000 pixel/s

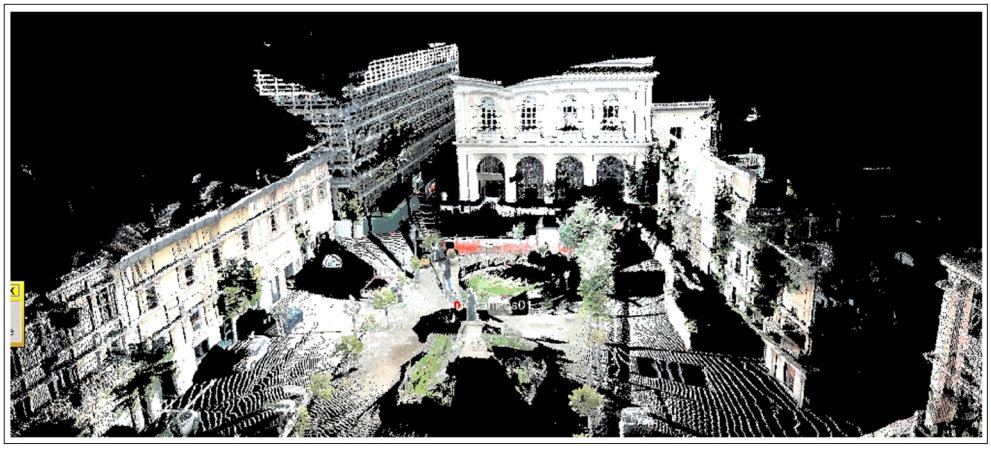

Figure 13 - LASER scanning survey acquired in the Piazza del Palazzo.

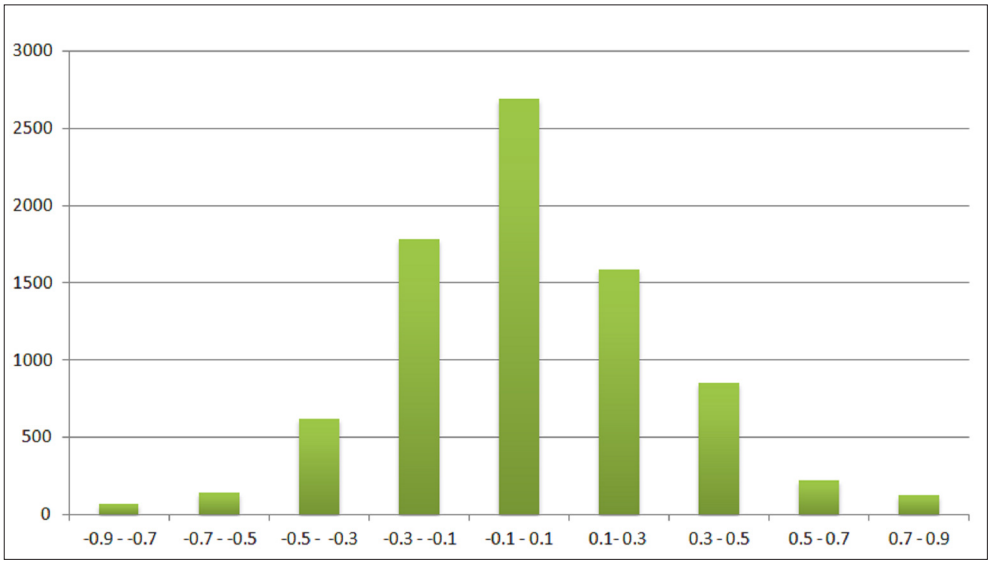

Figure 14 - Distribution of differences (m) between photogrammetric DSM and LASER points.

The slight systematic error that is observable can be attributed to the same causes of the previous comparisons: the presence or absence of vehicles and different response to foliage; it has also to be considered that trees can hide the ground for an extent that depends on the beam inclination [Barbarella et al., 2003]

After comparing the DSM with the LIDAR and LASER points, we also compared the LIDAR with the LASER acquisition to evaluate possible systematic shift. To perform the comparison, it was necessary to obtain a DSM from a LIDAR vector point (Fig. 15). The results obtained were then plotted in a histogram, shown in Figure 16. The comparisons show

a higher fit between LASER scanning and DSM by photogrammetry: this means that UAV DSM seems more accurate than LIDAR (Table 6). These results are quite promising because they imply that DSM meets the requirement for a large-scale map at 1:1000- 1:500.

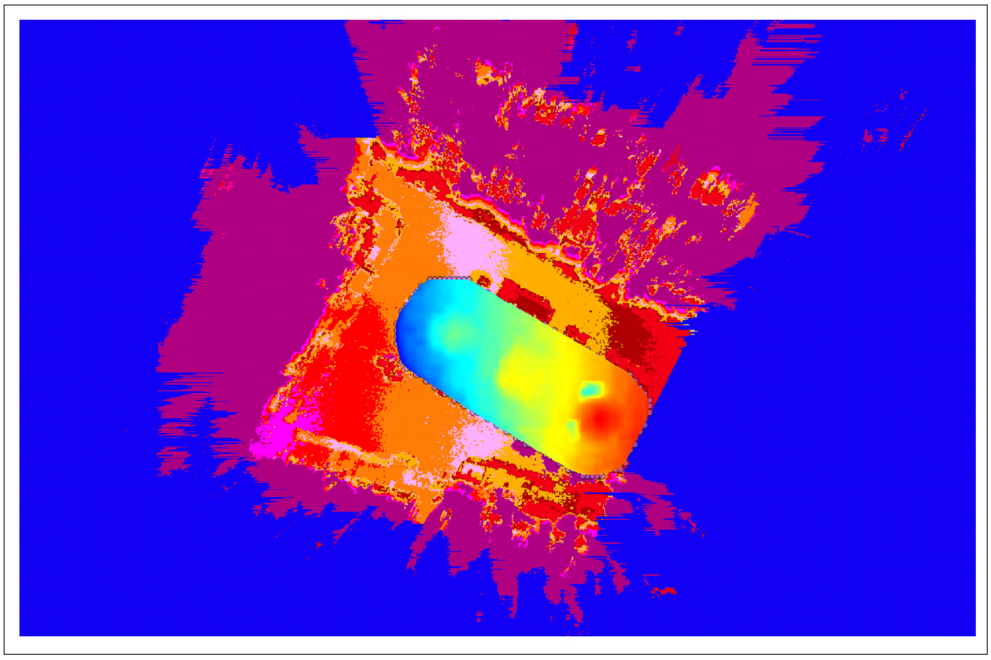

Figure - 15 DSM resulting from the LIDAR points.

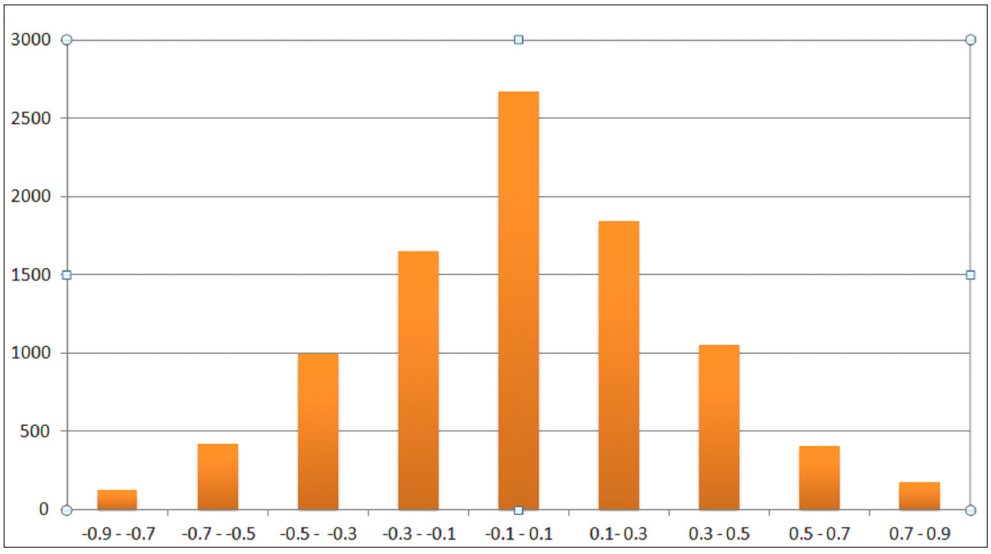

Figure 16 - Distribution of differences (m) between LIDAR and LASER points.

Unfortunately, in both cases, LIDAR and LASER, do not include the vegetation, this can be one possible cause of systematic errors when the photogrammetric DSM is compared with the LIDAR or LASER points cloud.

Table 6 - Statistic evaluation

	Mean	Absolute mean	Standard deviation
DSM - LIDAR	0.010197	0.416998	0.507456
LASER- DSM	0.008229	0.247164	0.314704
LIDAR - LASER	0.078025	0.273221	0.341521

Conclusion and further development

In this work, we evaluated some of the expected advantages of the use of UAVs in city centers for map updating, particularly in the case of difficult accessibility like in post-earthquake survey scenarios. We also evaluated how the optimization of flight planning can impact the stereoscopic reconstruction of an area of investigation. Initial results confirmed the geometric conditions hypothesized to automatically extract photogrammetric DSM, although further and more extensive tests must be performed. Several other tests in wider areas are presently in progress, and they will lead to a better evaluation of the accuracy. Anyway extraction of DSM from UAV imagery seems to report an impressive precision and a good accuracy. Presently, we can preliminarily estimate that the accuracy is near or perhaps higher than a classical LIDAR survey with a height accuracy of 0.15 m, but the time and cost advantages are still not evident, compared with more classical methodologies. A weak point, for instance, could be the need for a large number of GCPs; for example, in this test we used 21 differential GPS-acquired points; this because the limited payload of UAVs made impossible to install highly accurate navigation devices. In classical photogrammetry, as it is well known [Kraus, 1994], similar problems are solved using the bundle adjustment approach where a big number of tie points and a relative little number of GCPs is needed. So this approach will be fully experimented for acquisition like the one here illustrated in future works.

If three-dimensional clouds of points are available, also a SIFT (Scale Invariant Feature Transform) [Barazzetti et al., 2010; Bendea et al., 2008]approach can be experimented. Another similar approach currently under evaluation is based on the SFM (structure from motion) - MVF (multi-view stereo) [Kiparissi et al., 2012] algorithms but its results and accuracies are still under debate.

The correct planning of the acquisitions has demonstrated the importance of correctly reconstructing the proper geometry considering also the reduced autonomy of UAVs. A deeper investigation must be conducted to determine if a similar approach could be compatible with the instability observed in some UAV acquisitions. The tested algorithms will be also implemented in a graphical environment, like the available open source GIS, to facilitate the planning phase.

Acknowledgments
The authors would like to thank IPT company that gently provided the Microcopter survey.
This research was partially funded by MIUR (Italian Ministry for University and Research) with PRIN2008 and PRIN2010-2011 projects.

References

Alpen M., Frick K., Horn J. (2009) - *Nonlinear modeling and position control of an industrial quadrotor with on-board attitude control*. In: Proceedings of the IEEE International Conference on Control and Automation, ICCA, 2009',pp. 2329-2334.

Astrov I., Pedai A., Rustern E. (2010) - *Desired trajectory generation of a quadrotor helicopter using hybrid control for enhanced situational awareness*. In: Proceedings of the IEEE International Conference on Information and Automation (ICIA), pp. 1003-1007.

Baiocchi V., Dominici D., Milone M.V., Mormile M. (2013)- *Development of a software to plan UAVs stereoscopic flight: an application on post earthquake scenario in L'Aquila city*. Lecture Notes in Computer Science, 7974: 150-165. doi: http://dx.doi.org/10.2495/SAFE130111.

Baiocchi V., Dominici D., Mormile M. (2013) - *Unmanned Aerial Vehicle for post seismic and other hazard scenarios*. WIT Transactions on the Built Environment134: 113-122. doi:10.2495/SAFE130111.

Barazzetti, L., Remondino, F., Scaioni, M., Brumana, R. (2010) - *Fully Automatic Uav Image-Based Sensor Orientation*. In Proceeding.of ISPRS Commission I Mid-Term Symposium, Image Data Acquisition - Sensors & Platforms, 12.

Barbarella M., Fiani M. (2013) - *Monitoring of large landslides by Terrestrial Laser Scanning techniques: field data collection and processing.* European Journal of remote sensing, 46: 126-151. doi: http://dx.doi.org/10.5721/EuJRS20134608.

Barbarella, M., Gubellini, A., Russo P. (1984) - *Rilievo ed analisi dei recenti movimenti orizzontali del suolo nell'area Flegrea*. In: Atti del 2nd convegno del Gruppo Nazionale di Geofisica della Terra Solida, CNR, Roma, 2: 659-669.

Bendea, H., Boccardo, P., Dequal, S., Tonolo, F.G., Marenchino, D., Piras, M. (2008) - *Low cost UAV for post-disaster assessment*. The International Archives of the Photogrammetry, Remote Sensing and Spatial Information Sciences, XXXVII, (B8): 1373-1379.

Conte G., Doherty P., (2008) - *An Integrated UAV Navigation System Based on Aerial Image Matching*. In: Proceedings of the IEEE Aerospace Conference, pp. 1-10.

Costantino D., Angelini M.G. (2013) - *Production of DTM quality by TLS data*. European Journal of Remote Sensing, 46: 80-103. doi: http://dx.doi.org/10.5721/EuJRS20134606.

Eisenbeiss H., Haarbrink R.B. (2010) - *Accurate DSM production from unmanned helicopter systems*. ISPRS Technical Commission VII Symposium 100 Years ISPRS Advancing Remote Sensing Science, Vienna, Austria.

Erbil M.A., Prior S.D, Keane A.J. (2013) - *Design Optimization of a Reconfigurable Perching Element for Vertical Take-Off and Landing Unmanned Aerial Vehicles*. International Journal of Micro Air Vehicles, pp. 207-228.

Ercolin L., Julitta F., Montagna M., Rigon P., Sarazzi D. (2011) - *Moderne tecniche di*

rilievo aereo-fotogrammetrico di oggetti a sviluppo verticale per la produzione di DSM: il caso di Campione del Garda (BS). In: Proceedings symposyum ASITA 2011.

Eynard D., Vasseur P., Demonceaux C., Fremont V. (2010) - *UAV Motion Estimation using Hybrid Stereoscopic Vision*. MVA2011 IAPR Conference on Machine Vision Applications, Nara, JAPAN.

Eynard D., Demonceaux C., Vasseur P., Fremont V. (2011) - *UAV Motion Estimation using Hybrid Stereoscopic Vision*. MVA2011 IAPR Conference on Machine Vision Applications, Nara, JAPAN.

How J.P., Bethke B., Frank A., Dale D., Vian J. (2008) - *Real-time indoor autonomous vehicle test environment.* Transactions on IEEE Control Systems, pp. 51-64.

Hrabar S. (2008) - *3D Path Planning and Stereo-based Obstacle Avoidance for Rotorcraft UAVs*. 2008 IEEE/RSJ International Conference on Intelligent Robots and Systems Acropolis Convention Center Nice, France. doi: http://dx.doi.org/10.1109/IROS.2008.4650775.

Hrabar S. (2008) - *3D path planning and stereo-based obstacle avoidance for rotorcraft UAVs*. In: Proceedings of the IEEE/RSJ International Conference on Intelligent Robots and Systems (IROS), 2008, pp. 807-814.

Kiparissi S., Skarlatos D. (2012) - *Comparison of laser scanning, photogrammetry and sfm-mvspipeline applied in structures and artificial surfaces*. ISPRS Annals of the Photogrammetry, Remote Sensing and Spatial Information Sciences, I-3, XXII ISPRS Congress, 25 August - 01 September 2012, Melbourne, Australia.

Ioannis K. Nikolos, Kimon P. Valavanis, Senior Member, Nikos C. Tsourveloudis, and Anargyros N. Kostaras (2003) - *Evolutionary Algorithm Based Offline/Online Path Planner for UAV Navigation.* IEEE transactions on systems, man, and cybernetics-part b: cybernetics, 33 (6). doi: http://dx.doi.org/10.1109/TSMCB.2002.804370.

Kraus K. (1994) - *Photogrammetry*. Politecnico di Torino Cap 3: 147-153.

Lim H., Park J., Lee D., Kim H. (2012) - *Open-Source Projects for Quadrotor Unmanned Aerial Vehicles*. IEEE Robotics and Automation Magazine, 19 (3): 33-45. doi: http://dx.doi.org/10.1109/MRA.2012.2205629.

Mellinger D., Kumar V. (2011) - *Minimum snap trajectory generation and control for quadrotors*. In: Proceedings of the IEEE International Conference on Robotics and Automation (ICRA), pp. 2520-2525.

Moore R.J.D., Thurrowgood S., Bland D., Mandyam V. Srinivasan (2010) - *UAV Altitude and Attitude Stabilisation using a Coaxial Stereo Vision System*. IEEE International Conference on Robotics and Automation Anchorage Convention District, Anchorage, Alaska, USA.

Neininger B., Hacker J.M. (2011) - *Manned or unmanned – does this really matter?*. International Archives of the Photogrammetry, Remote Sensing and Spatial Information Sciences, XXXVIII-1/C22 UAV-g, Conference on Unmanned Aerial Vehicle in Geomatics, Zurich, Switzerland.

Nex, Francesco, Fabio Remondino (2013) - *UAV for 3D mapping applications: A review*. Applied Geomatics, pp. 1-15.

Nikolos I.K, Valavanis K.P., Tsourveloudis N.C., Kostaras A.N. (2003) - *Evolutionary algorithm based offline/online path planner for UAV navigation*. IEEE transactions on Systems, Man, and Cybernetics, Part B: Cybernetics, pp. 898-912. doi: http://dx.doi.

org/10.1109/TSMCB.2002.804370.

Nikolos I.K., Valavanis K.P., Tsourveloudis N.C., Kostaras A.N. (2013) - *Evolutionary Algorithm Based Offline/Online Path Planner for UAV Navigation*. IEEE transactions on systems, man, and cybernetics-part b: cybernetics, 33 (6).

Novelli V.I., D'Ayala D. (2012) - *Assessment of the most damaged historic centres of the Region Emilia Romagna due to the earthquake of the 20th and 29th of May 2012*. Ingegneria Sismica, 29 (2-3): 59-71.

Rathbun D., Kragelund S., Pongpunwattana A., Capozzi B. (2002) - *An evolution based path planning algorithm for autonomous motion of a UAV through uncertain environments*. In: Proceedings of the 21st Digital Avionics Systems Conference, 8D2-1-8D2-12 (2).

Stefanik K.V., Gassaway J.C., Kochersberger K., Abbott A.L. (2011) - *UAV-Based Stereo Vision for Rapid Aerial Terrain Mapping*. GIScience & Remote Sensing, 48, (1): 24-49. doi: http://dx.doi.org/10.2747/1548-1603.48.1.24.

Xiong H., Yuan R., Jianqiang J., Fan G., Jing F. (2011) - *Disturbance Rejection in UAV's velocity and attitude control: Problems and solutions*. In: Proceedings of the 30th Chinese Control Conference (CCC), pp. 6293-6298.